Medicinal Chemistry Hot Paper

DOI: 10.1002/ange.201409043

Design and Synthesis of High-Affinity Dimeric Inhibitors Targeting the Interactions between Gephyrin and Inhibitory Neurotransmitter Receptors

*Hans Michael Maric, Vikram Babu Kasaragod, Linda Haugaard-Kedström, Torben Johann Hausrat, Matthias Kneussel, Hermann Schindelin, and Kristian Strømgaard**

Abstract: *Gephyrin is the central scaffolding protein for inhibitory neurotransmitter receptors in the brain. Here we describe the development of dimeric peptides that inhibit the interaction between gephyrin and these receptors, a process which is fundamental to numerous synaptic functions and diseases of the brain. We first identified receptor-derived minimal gephyrin-binding peptides that displayed exclusive binding towards native gephyrin from brain lysates. We then designed and synthesized a series of dimeric ligands, which led to a remarkable 1220-fold enhancement of the gephyrin affinity ($K_D = 6.8$ nM). In X-ray crystal structures we visualized the simultaneous dimer-to-dimer binding in atomic detail, revealing compound-specific binding modes. Thus, we defined the molecular basis of the affinity-enhancing effect of multivalent gephyrin inhibitors and provide conceptually novel compounds with therapeutic potential, which will allow further elucidation of the gephyrin–receptor interplay.*

The primary inhibitory neurotransmitter receptors, namely glycine receptors (GlyRs)[1] and γ-aminobutyric acid type A receptors ($GABA_A$Rs), are accumulated at post-synaptic sites in the brain[2] by the scaffolding protein gephyrin through direct interactions.[3] Accordingly, knockout of gephyrin in mice is accompanied by loss of receptor clusters and is lethal.[2e,4]

Gephyrin interacts with GlyRs and $GABA_A$Rs via a universal binding site[2b] located within the gephyrin E domain (GephE),[5] although distinct GlyR and $GABA_A$R interactions have very recently been described.[6] The affinity of the gephyrin–receptor interaction depends on the oligomeric state of gephyrin and the number of gephyrin-binding receptor subunits in the functional receptor.[7] Consequently, the oligomerization of gephyrin, GlyRs, and $GABA_A$Rs are interdependent.[4b,8]

Dysregulation of $GABA_A$R-mediated neurotransmission, in particular, has been implicated in a wide range of disorders in the brain.[9] Accordingly, compounds targeting $GABA_A$Rs have been extensively explored and are in widespread clinical use.[10] In the search for improved drugs with potentially novel indications, there has been a substantial, but so far unsuccessful effort directed towards the development of compounds with improved receptor-subtype selectivity.[11]

As a conceptually different approach, one could target the interaction between the $GABA_A$R and its intracellular scaffolding protein gephyrin. This is substantiated by the fact that GlyR and $GABA_A$R functions are markedly affected by gephyrin-binding-deficient mutations.[2a–d] Additionally, in a principally similar approach, compounds with great therapeutic promise have been developed for other interactions between receptors and scaffolding proteins.[12] We envision that receptor-derived peptides function as templates to generate high-affinity ligands that could modulate the gephyrin–receptor interaction in vivo and potentially have therapeutic relevance.[13] Importantly, such molecules could help decipher $GABA_A$R and GlyR population dynamics,[14] which, so far, have remained poorly defined due to the lack of tools for acutely and specifically controlling the underlying gephyrin-binding interactions.[15] Here we present the design and synthesis of dimeric peptide ligands that target gephyrin with a remarkable specificity and display unprecedented high affinity towards gephyrin and hence could open a new pathway to modulate inhibitory synaptic transmission (Figure 1).

Our initial aim was to identify short receptor-derived peptides that display specific gephyrin binding, and subsequently use the optimized monomeric peptides as templates in the design of dimeric peptide ligands. First, we performed a systematic structure–activity relationship (SAR) study of monovalent peptides derived from either the β subunit of the GlyR (peptides **1a**–**v**) or from the α3 subunit of the $GABA_A$R (peptides **1w**–**z**). The affinity of these peptides to recombinantly expressed GephE was determined using isothermal titration calorimetry (ITC) data for the dissociation constants (Table 1) as well as binding enthalpy and entropy (Table S1 and Figures S1 and S2).

The 50-residue GlyR fragment **1a** that displays wild-type gephyrin affinity[1a] with a K_D of (2.1 ± 0.5) μM was used as a reference. Shorter peptide sequences were chosen on the

[*] Dr. H. M. Maric, Dr. L. Haugaard-Kedström, Prof. Dr. K. Strømgaard
Department of Drug Design and Pharmacology
University of Copenhagen
Universitetsparken 2, 2100 Copenhagen (Denmark)
E-mail: kristian.stromgaard@sund.ku.dk
V. B. Kasaragod, Prof. Dr. H. Schindelin
Institute of Structural Biology, Rudolf Virchow Center for Experimental Biomedicine, University of Würzburg
Josef-Schneider-Strasse 2, 97080 Würzburg (Germany)
Dr. T. J. Hausrat, Prof. Dr. M. Kneussel
Department of Molecular Neurogenetics
Center for Molecular Neurobiology
ZMNH, University Medical Center
Hamburg-Eppendorf, 20251 Hamburg (Germany)

Supporting information for this article is available on the WWW under http://dx.doi.org/10.1002/anie.201409043.

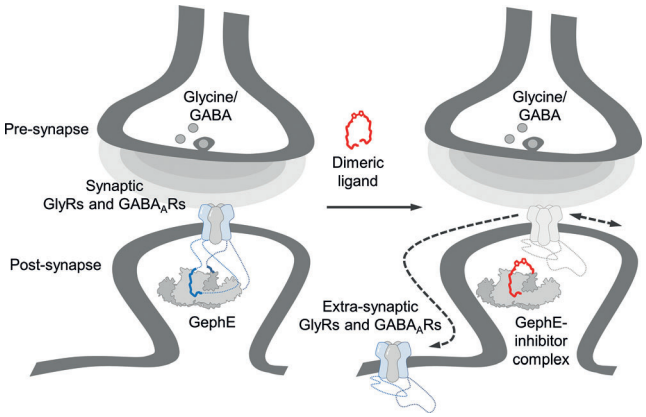

Figure 1. Principle action of dimeric gephyrin inhibitors on the synaptic localization of GlyRs and GABA$_A$Rs. GABA$_A$Rs and GlyRs are concentrated at synaptic sites via a direct interaction of their large intracellular loops with an overlapping gephyrin binding site. The receptor-binding C-terminal gephyrin E domain (GephE) dimerizes and offers two receptor binding sites in close proximity. Dimeric ligands could simultaneously target two receptor binding sites and thereby interfere with the accumulation of a specific subset of the receptors at postsynaptic sites by competition, thus acting as modulators of GABAergic and glycinergic transmission.

Table 1: Identification of minimal gephyrin-specific peptides. Shown are the peptides **1a–z**, their residue numbers, sequences, and dissociation constants (K_D) obtained from ITC by titration against GephE. Phe398 and Pro405 are shown in red and mark the borders of the minimal binding peptide.

No.	AA	Sequence	K_D [μM]
1a	50	^{377}H$_2$N-...F S I V G S L P R D F E L S...-COOH^{426}	2.1 ± 0.5
1b	14	^{398}H$_2$N-F S I V G S L P R D F E L S-COOH^{411}	6 ± 2
1c	13	^{398}H$_2$N-F S I V G S L P R D F E L-COOH^{410}	4.5 ± 0.2
1d	12	^{398}H$_2$N-F S I V G S L P R D F E-COOH^{409}	13 ± 7
1e	11	^{398}H$_2$N-F S I V G S L P R D F-COOH^{408}	8.3 ± 0.1
1f	10	^{398}H$_2$N-F S I V G S L P R D-COOH^{407}	15 ± 4
1g	09	^{398}H$_2$N-F S I V G S L P R-COOH^{406}	19 ± 18
1h	08	^{398}H$_2$N-F S I V G S L P-COOH^{405}	20 ± 4
1i	07	^{398}H$_2$N-F S I V G S L-COOH^{404}	> 500
1j	06	^{398}H$_2$N-F S I V G S-COOH^{403}	> 500
1k	05	^{398}H$_2$N-F S I V G-COOH^{402}	> 500
1l	11	^{398}H$_2$N-A S I V G S L P R D F-COOH^{408}	> 500
1m	11	^{398}H$_2$N-F S I V G S L A R D F-COOH^{408}	42 ± 22
1n	11	^{398}H$_2$N-A S I V G S L A R D F-COOH^{408}	> 500
1o	11	^{398}H$_2$N-A S A V G S L A R D F-COOH^{408}	> 500
1p	06	^{398}H$_2$N-F S I V G S-CONH$_2$^{403}	> 500
1q	07	^{398}H$_2$N-F S I V G S L-CONH$_2$^{403}	> 500
1r	08	^{398}H$_2$N-F S I V G S L P-CONH$_2$^{405}	8.9 ± 0.3
1s	07	^{399}H$_2$N-S I V G S L P-CONH$_2$^{405}	> 500
1t	09	^{397}H$_2$N-D F S I V G S L P-CONH$_2$^{405}	71 ± 20
1u	10	^{396}H$_2$N-N D F S I V G S L P-CONH$_2$^{405}	69 ± 18
1v	11	^{395}H$_2$N-S N D F S I V G S L P-CONH$_2$^{405}	79 ± 7
1w	11	^{370}H$_2$N-F N I V G T T Y P I N-COOH^{380}	190 ± 30[a]
1x	10	^{370}H$_2$N-F N I V G T T Y P I-COOH^{379}	221 ± 34[a]
1y	9	^{370}H$_2$N-F N I V G T T Y P-COOH^{378}	253 ± 38[a]
1z	8	^{370}H$_2$N-F N I V G T T Y-COOH^{377}	> 500[a]

[a] **1w–z** were measured and analyzed previously.[6]

basis of earlier mutagenesis and structural studies.[1a,b,2b,5,6,7] Truncation of **1a** to a 14-residue core binding peptide (**1b**), which could be resolved in a X-ray crystal structure,[5] resulted in a roughly threefold weaker affinity ($K_D = (6 \pm 2)$ μM). From peptide **1b** a range of modifications were made in order to identify a truncated peptide with good affinity to GephE; the modifications included C-terminal truncations **1c–k**, point mutations **1l–o**, truncated amide variants **1p–r**, and N-terminally elongated amide variants **1s–v**. This SAR study additionally provided a number of key features for gephyrin binding, which are described in the Supporting Information, and identified an octapeptide ligand **1r** which retains roughly 90% of the free energy upon binding GephE when compared to the 50-mer peptide **1a**.

Having identified truncated peptides displaying a high affinity for recombinant GephE, we were interested in assessing the affinity and specificity for native full-length gephyrin. We employed an affinity-based approach, where the identified peptides were challenged with a murine whole-brain homogenate, representing a highly complex gephyrin-containing matrix. Peptides **1c–k** were covalently immobilized on iodoacetyl-activated beads and subsequently incubated with mouse whole-brain lysate (Figure 2). Satisfyingly,

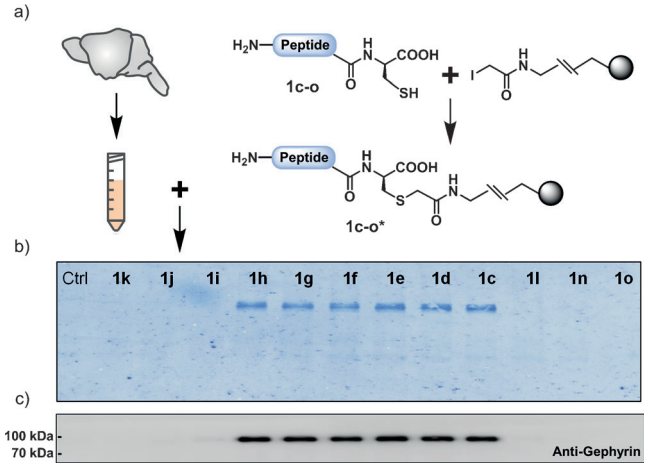

Figure 2. Short GlyR-derived peptides bind native gephyrin. a) Scheme of the pull-down of native gephyrin. Whole mouse brain lysate was freshly prepared and GlyR-derived peptides **1c–k** as well as mutated variants **1l–o** were immobilized using iodoacetyl reactive resin. b) The Coomassie-stained gel revealed that peptides **1c–h** exclusively bind gephyrin, while the Ala mutants **1l–o** and 5- and 6-residue wild-type variants **1k** and **1j** did not. c) Immune detection verified the identity of gephyrin.

there was an excellent correlation between the in vitro ITC data and the ability to recover native gephyrin from mouse brain: The six peptides **1c–h**, but not peptides **1i–k**, bind gephyrin, as visualized by western blot (Figure 2c). Importantly, a Coomassie-stained gel of the same resin-bound peptides (Figure 2b) demonstrates a remarkably high specificity of the peptides for native gephyrin. Thus, the peptides interact with gephyrin from mouse brain with high efficiency.

Next, we employed the identified monomeric peptides in the design and synthesis of dimeric ligands, which we envisioned to simultaneously bind to the dimeric GephE domain, thereby enhancing affinity and acting as potent inhibitors of this interaction. Specifically, GlyR-derived

peptides **1c–h** and $GABA_AR$-derived peptides **1w–y** were dimerized using various linkers. Since the N-terminal regions of these peptides were presumed to display important interaction points with gephyrin, the dimeric peptide ligands were synthesized by C-terminal dimerization. Linker moieties with variations in hydrophobicity, length, and flexibility were employed, and systematically combined with the different peptide ligands. Specifically, rigid phenyl-based linkers **2a–c**, short alkyl linkers **2d**, and longer flexible poly(ethylene glycol) (PEG)-based linkers **2e** were used to dimerize peptides **1e–y**, which varied in length between 8 and 13 residues, yielding 25 different dimeric peptides **3a–y** (Figure 3a and Figure S3). The dimeric peptides were evaluated for their affinity to recombinant GephE using ITC (Figure 3b–d, Figures S2, S4, and S5, and Table S1). Gratifyingly, all dimeric ligands displayed a significant increase in affinity compared to the corresponding monomeric peptide. The potentiation of affinity upon dimerization followed two basic principles: 1) The nature of the linker determines the overall affinity of dimeric peptides, with PEG being the best and *m*-phenyl the worst linker; 2) the length and not the affinity of the peptide ligands determine the gephyrin-binding potency over a range of more than one order of magnitude, with 11 residues being optimal. The synergistic effect of linker and peptide optimization together led to a 1220-fold improved binding affinity of dimeric ligand **3m** with a K_D of (6.8 ± 0.6) nM compared to the corresponding monovalent peptide **1e** ($K_D = (8.3 \pm 0.1)$ μM). We also extended the concept to the $GABA_AR$ α3 subunit derived peptides, which display the highest gephyrin affinity among all $GABA_AR$ subunit peptides analyzed so far. Here, dimerization yielded a K_D of (288 ± 86) nM, corresponding to an 880-fold increase in affinity, similar to the best GlyR-derived dimeric fragment. Evaluation of the mutated dimeric ligands **3x–z** excluded contributions to the affinity by the linker region and therefore the observed affinity potentiation is solely based on the simultaneous binding of both peptide ligands.

From the ITC experiments, we found that the dimeric peptide ligands bind with a 1:2 stoichiometry to GephE, in line with the simultaneous binding of both peptide moieties to dimeric GephE. This was confirmed by analytical size-exclusion chromatography (SEC) and multi-angle light scattering (MALS) which both clearly demonstrated the dimeric oligomerization state of GephE in the presence and absence of the dimeric ligands (Figure S6).

To elucidate the binding mode of the dimeric peptides to GephE, we determined the X-ray crystal structures of two dimeric ligands at a resolution of 2 Å: The dimeric ligand **3v** containing a flexible PEG linker and a $GABA_AR$-derived peptide, and the dimeric ligand **3d** with shorter GlyR-derived peptides and a rigid phenyl-based linker. The X-ray crystal structures of GephE in complex with **3v** (PDB ID: 4U90) (Figure 4a–c) and **3d** (PDB ID: 4U91) (Figure 4d–f) illustrate how both peptide ligands engage simultaneously with two GephE monomers, which, however, belong to different dimers, and how the supramolecular complex between GephE and the dimeric peptide is spatially arranged (Figure S7).

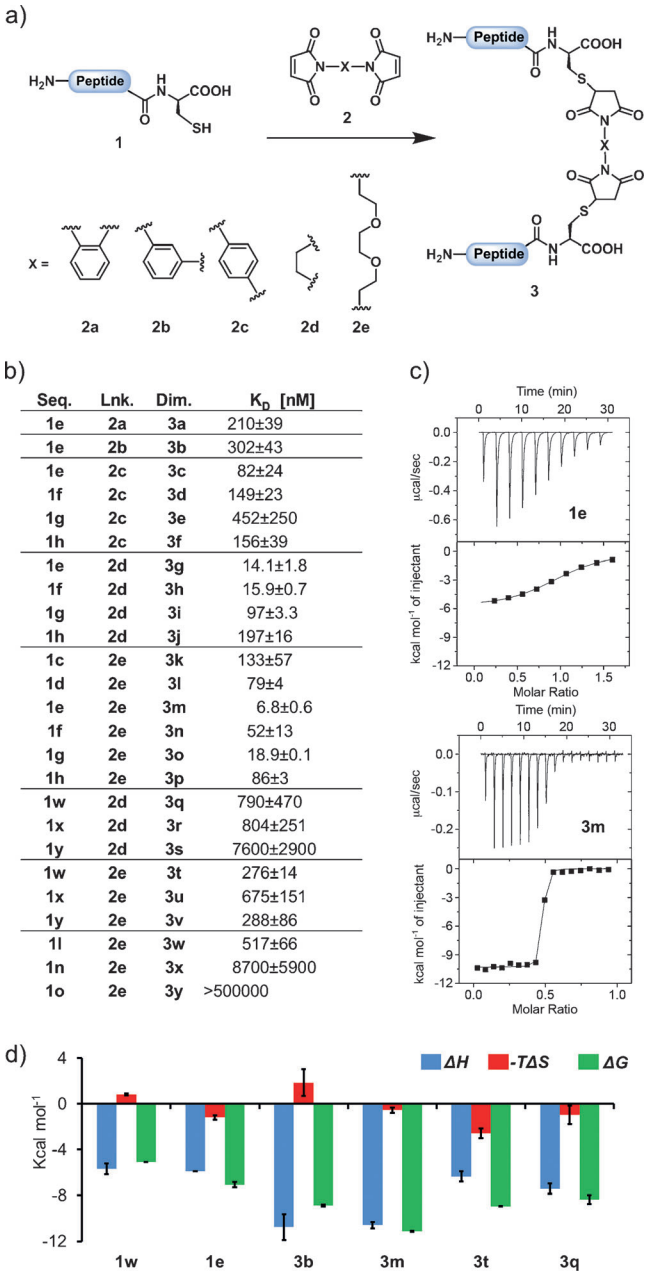

Seq.	Lnk.	Dim.	K_D [nM]
1e	2a	3a	210±39
1e	2b	3b	302±43
1e	2c	3c	82±24
1f	2c	3d	149±23
1g	2c	3e	452±250
1h	2c	3f	156±39
1e	2d	3g	14.1±1.8
1f	2d	3h	15.9±0.7
1g	2d	3i	97±3.3
1h	2d	3j	197±16
1c	2e	3k	133±57
1d	2e	3l	79±4
1e	2e	3m	6.8±0.6
1f	2e	3n	52±13
1g	2e	3o	18.9±0.1
1h	2e	3p	86±3
1w	2d	3q	790±470
1x	2d	3r	804±251
1y	2d	3s	7600±2900
1w	2e	3t	276±14
1x	2e	3u	675±151
1y	2e	3v	288±86
1l	2e	3w	517±66
1n	2e	3x	8700±5900
1o	2e	3y	>500000

Figure 3. Design and synthesis of dimeric peptides and their in vitro binding properties. a) Monomeric GlyR β derived **1c–o** or $GABA_AR$ α3 derived **1w–y** peptides were dimerized in solution via a C-terminally added Cys, which reacted with different bismaleamide-containing linkers **2a–e** to yield their dimeric variants **3a–y**. b) Dissociation constants of dimeric compounds **3a–y** determined by ITC together with their linker type **2a–e** and their peptide sequence **1e–y**. c) Representative ITC diagrams of the monovalent peptide **1e** and its dimeric variant **3m**. d) Thermodynamic bar graphs for selected compounds.

Since our MALS data (Figure S6) demonstrated that each dimeric ligand binds to just one GephE dimer, the binding modes observed in the two crystal structures (Figure 4 and Figure S7) represent interesting examples of domain swapping.[16] Despite the different domain-swapped arrangements, all receptor binding sites are occupied in both structures.

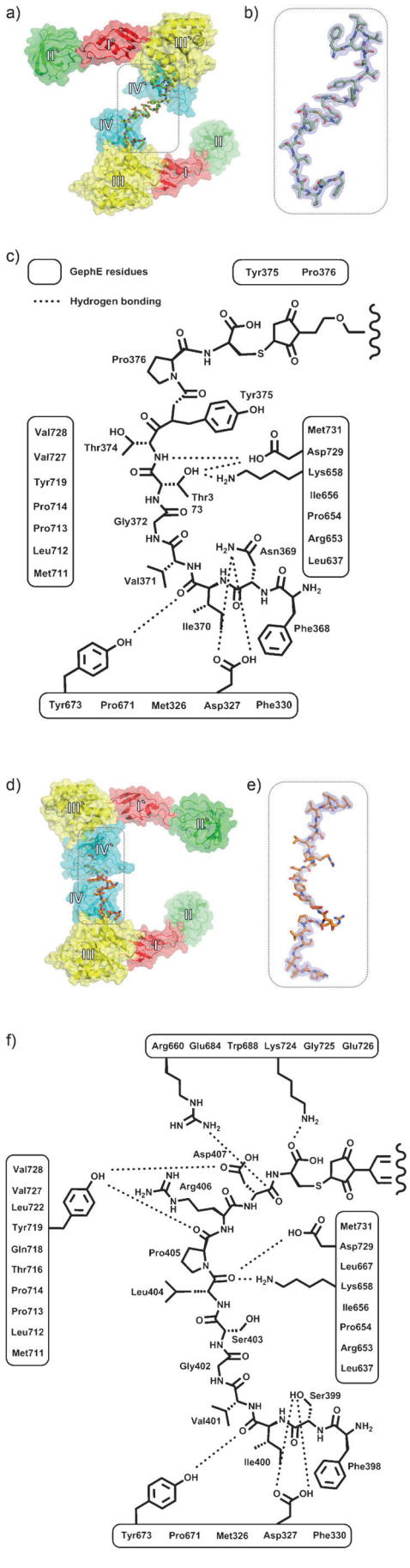

In both structures the peptide binding pocket is mainly created by GephE subdomain IV and partially by subdomain III (Figure 4a,d), which acts as universal binding site for the GlyR β and $GABA_AR$ α subunit derived peptides.[2b] Nonetheless, both compounds also engage in unique GephE interactions (Figure 4c,f). Remarkably, the linkers of the PEG-based **3v** and the phenyl-based **3d** dimeric ligands are fully resolved in the electron density maps (Figure 4b,e), indicating a tight and rigid arrangement of both linkers. Due to the high resolution, the cocrystal structure of the $GABA_AR$ α3 derived peptide **3v** also reveals new features, which are described in the Supporting Information.

Peptide-based ligands are generally subject to enzymatic cleavage by proteases in vivo, which often is the major limiting factor for advanced biological studies. We therefore evaluated the stability of selected monomeric and dimeric peptide ligands in an in vitro serum stability assay (Figure S8). In contrast to the monomeric peptides **1x–w**, which were degraded relatively fast with half-lives ($t_{1/2}$) of 4–6 min, the dimeric ligands **3q,r** and **3t,u** comprising different linkers displayed a 24- to 41-fold increase in stability, with a maximal $t_{1/2}$ of more than 4 h (Figure S8). Thus, dimerization of peptide ligands leads to stability superior to that of standard, monomeric peptides.[12e]

In conclusion, we first identified short gephyrin-binding peptides with moderate affinity, which, however, displayed exclusive and efficient binding to native gephyrin. Dimerization of these peptide ligands with different linkers led to dimeric ligands that target gephyrin with unprecedented high affinity, with the most potent ligand displaying an affinity in the low nanomolar range. Additionally, dimerization also substantially improved the serum stability, thus providing compounds with great promise for further studies of gephyrin–receptor interactions. Finally, the atomic details of the interaction between the dimeric ligands and gephyrin was revealed by X-ray crystallography, showing several interesting features including that both peptide ligands engage with two GephE proteins simultaneously and in distinct binding modes.

It is known that GABAergic transmission can be modulated by changing the lateral diffusion of $GABA_ARs$[17] and that small peptide fragments can effectively compete with the full-length intracellular receptor loops.[2b,7] Accordingly, the compounds presented here likely target the anchoring of a defined subset of $GABA_AR$ and GlyR receptors, namely receptors that rely on gephyrin-mediated anchoring such as $GABA_ARs$ containing the α1[2a] or α3[2d] subunits and GlyRs

Figure 4. X-ray crystallographic analyses of two GephE complexes with dimeric peptides. a) Binding of the $GABA_AR$ α3 derived PEG-linked dimeric peptide **3v** in stick representation (PDB ID: 4U90) to GephE. Subdomains 1–4 are indicated by Roman numbers and colored differently. b) Stick model and feature-enhanced electron density map (FEM) at one times the root mean square deviation for the bound dimeric peptide **3v**. c) Detailed 2D representation of the GephE interactions of one half of the dimeric peptide **3v**. d) Structure of **3d**, a GlyR β derived *p*-phenyl-linked dimeric peptide, engaging with two GephE proteins molecules simultaneously (PDB ID: 4U91). e) Stick model and FEM of **3d** bound to GephE. f) 2D representation of one half of the GephE–**3d** complex.

featuring the β subunit (Figure 1).[1a] We speculate that these molecules could: 1) Act as highly receptor-subtype-specific functional antagonists by uncoupling receptors from synaptic sites and hence decrease fast-synaptic inhibition. 2) Function as subtype-specific functional agonists, by accelerating the exchange rate of desensitized receptors at post-synaptic sites.[18] Such subtype-specific $GABA_AR$ agonists hold promise to overcome the limitations of classical benzodiazepines.[11] 3) Shift the balance of phasic inhibition, mediated by post-synaptic receptors, to tonic inhibition, mediated by extra-synaptic receptors. Extra-synaptic $GABA_ARs$ are considered to hold great potential as therapeutic targets.[9,19]

Received: September 12, 2014
Published online: November 24, 2014

Keywords: calorimetry · drug design · medicinal chemistry · structural biology · structure–activity relationship

[1] a) G. Meyer, J. Kirsch, H. Betz, D. Langosch, *Neuron* **1995**, *15*, 563 – 572; b) M. Kneussel, A. Hermann, J. Kirsch, H. Betz, *J. Neurochem.* **1999**, *72*, 1323 – 1326; c) C. Maas, N. Tagnaouti, S. Loebrich, B. Behrend, C. Lappe-Siefke, M. Kneussel, *J. Cell. Biol.* **2006**, *172*, 441 – 451.

[2] a) J. Mukherjee, K. Kretschmannova, G. Gouzer, H. M. Maric, S. Ramsden, V. Tretter, K. Harvey, P. A. Davies, A. Triller, H. Schindelin, S. J. Moss, *J. Neurosci.* **2011**, *31*, 14677 – 14687; b) H. M. Maric, J. Mukherjee, V. Tretter, S. J. Moss, H. Schindelin, *J. Biol. Chem.* **2011**, *286*, 42105 – 42114; c) V. Tretter, T. C. Jacob, J. Mukherjee, J. M. Fritschy, M. N. Pangalos, S. J. Moss, *J. Neurosci.* **2008**, *28*, 1356 – 1365; d) V. Tretter, B. Kerschner, I. Milenkovic, S. L. Ramsden, J. Ramerstorfer, L. Saiepour, H. M. Maric, S. J. Moss, H. Schindelin, R. J. Harvey, W. Sieghart, K. Harvey, *J. Biol. Chem.* **2011**, *286*, 37702 – 37711; e) M. Kneussel, J. H. Brandstätter, B. Laube, S. Stahl, U. Müller, H. Betz, *J. Neurosci.* **1999**, *19*, 9289 – 9297.

[3] X. Wu, Z. Wu, G. Ning, Y. Guo, R. Ali, R. L. Macdonald, A. L. De Blas, B. Luscher, G. Chen, *J. Biol. Chem.* **2012**, *287*, 27417 – 27430.

[4] a) G. Feng, H. Tintrup, J. Kirsch, M. C. Nichol, J. Kuhse, H. Betz, J. R. Sanes, *Science* **1998**, *282*, 1321 – 1324; b) C. Essrich, M. Lorez, J. A. Benson, J. M. Fritschy, B. Luscher, *Nat. Neurosci.* **1998**, *1*, 563 – 571.

[5] E. Y. Kim, N. Schrader, B. Smolinsky, C. Bedet, C. Vannier, G. Schwarz, H. Schindelin, *EMBO J.* **2006**, *25*, 1385 – 1395.

[6] H. M. Maric, V. B. Kasaragod, J. T. Hausrat, V. Tretter, M. Kneussel, K. Strømgaard, H. Schindelin, *Nat. Commun.* **2014**, in press.

[7] H. M. Maric, V. B. Kasaragod, H. Schindelin, *ACS Chem. Biol.* DOI: DOI: 10.1021/cb500303a.

[8] A. Vlachos, S. Reddy-Alla, T. Papadopoulos, T. Deller, H. Betz, *Cereb. Cortex* **2013**, *23*, 2700 – 2711.

[9] R. M. Hines, P. A. Davies, S. J. Moss, J. Maguire, *Curr. Opin. Neurobiol.* **2012**, *22*, 552 – 558.

[10] G. A. Johnston, *Pharmacol. Ther.* **1996**, *69*, 173 – 198.

[11] U. Rudolph, F. Knoflach, *Nat. Rev. Drug Discovery* **2011**, *10*, 685 – 697.

[12] a) M. Sainlos, W. S. Iskenderian-Epps, N. B. Olivier, D. Choquet, B. Imperiali, *J. Am. Chem. Soc.* **2013**, *135*, 4580 – 4583; b) M. Sainlos, C. Tigaret, C. Poujol, N. B. Olivier, L. Bard, C. Breillat, K. Thiolon, D. Choquet, B. Imperiali, *Nat. Chem. Biol.* **2011**, *7*, 81 – 91; c) C. N. Chi, A. Bach, K. Strømgaard, S. Gianni, P. Jemth, *Biofactors* **2012**, *38*, 338 – 348; d) A. Bach, B. H. Clausen, M. Møller, B. Vestergaard, C. N. Chi, A. Round, P. L. Sørensen, K. B. Nissen, J. S. Kastrup, M. Gajhede, P. Jemth, A. S. Kristensen, P. Lundström, K. L. Lambertsen, K. Strømgaard, *Proc. Natl. Acad. Sci. USA* **2012**, *109*, 3317 – 3322; e) A. Bach, C. N. Chi, G. F. Pang, L. Olsen, A. S. Kristensen, P. Jemth, K. Strømgaard, *Angew. Chem. Int. Ed.* **2009**, *48*, 9685 – 9689; *Angew. Chem.* **2009**, *121*, 9865 – 9869.

[13] a) E. Dolgin, *Nat. Med.* **2012**, *18*, 1003 – 1006; b) A. Flemming, *Nat. Rev. Drug Discovery* **2012**, *11*, 272.

[14] C. G. Specht, I. Izeddin, P. C. Rodriguez, M. El Beheiry, P. Rostaing, X. Darzacq, M. Dahan, A. Triller, *Neuron* **2013**, *79*, 308 – 321.

[15] a) S. K. Tyagarajan, J. M. Fritschy, *Nat. Rev. Neurosci.* **2014**, *15*, 141 – 156; b) V. Tretter, J. Mukherjee, H. M. Maric, H. Schindelin, W. Sieghart, S. J. Moss, *Front. Cell. Neurosci.* **2012**, *6*, 23.

[16] A. M. Gronenborn, *Curr. Opin. Struct. Biol.* **2009**, *19*, 39 – 49.

[17] A. Triller, D. Choquet, *Trends Neurosci.* **2005**, *28*, 133 – 139.

[18] a) M. Heine, L. Groc, R. Frischknecht, J. C. Beique, B. Lounis, G. Rumbaugh, R. L. Huganir, L. Cognet, D. Choquet, *Science* **2008**, *320*, 201 – 205; b) E. M. Petrini, J. Lu, L. Cognet, B. Lounis, M. D. Ehlers, D. Choquet, *Neuron* **2009**, *63*, 92 – 105.

[19] S. G. Brickley, I. Mody, *Neuron* **2012**, *73*, 23 – 34.

